

The behaviour and function of bottle cells during gastrulation of *Xenopus laevis*

JEFF HARDIN^{1,*} and RAY KELLER²

¹Biophysics and Medical Physics Group and ²Department of Zoology, University of California, Berkeley, CA 94720, USA

Present address: Department of Zoology, Duke University, Durham, North Carolina, 27706, USA

Summary

The behaviour of bottle cells in normal and microsurgically altered gastrulae and in cultured explants of *Xenopus laevis* was analysed, using time-lapse micrography, scanning electron microscopy (SEM) and cell tracing with fluorescein dextran amine (FDA). The results shed new light on the function of bottle cells. Bottle cells forming *in vivo* show a predominantly animal–vegetal apical contraction and a concurrent apical–basal elongation, whereas those forming in cultured explants show uniform apical contraction and remain rotund. Bottle cells forming in embryos with fewer subblastoporal cells contract more uniformly than those in normal embryos and release of normal bottle cells from supra- and subblastoporal cells results in immediate loss of the bottle shape. These results, and an analysis of the effects of bottle cell formation on the shapes and movements of surrounding tissues, show that unique shape of bottle cells

and their probable function in development are not intrinsic properties but result from a modulation of the effect of a uniform and intrinsic apical contraction by the geometric and mechanical properties of the surrounding tissue. Mechanical simulations of bottle cell formation, using the finite element method, suggest how the site of bottle cell formation and the thickness and stiffness of adjacent tissues might change the effects of their formation. These results and FDA marking of prospective bottle cells and the adjacent deep mesodermal cells suggest that bottle cells function during their formation to initiate the involution of the prospective mesodermal mantle. Later they respread to deepen the archenteron and to form its peripheral wall.

Key words: invagination, bottle cells, gastrulation, *Xenopus*.

Introduction

The unique shape of the ‘bottle’ or ‘flask’ cells and their position at the site of blastopore formation suggested to early embryologists that they must play a major role in the gastrulation of amphibians (Rhumbler, 1902; Ruffini, 1925). There are two not mutually exclusive notions of how these cells function in gastrulation. Rhumbler (1902) & Holtfreter (1943*a,b*) argued that bottle cells invade the interior of the gastrula because the alkaline environment there (Buytendijk & Woerdeman, 1927; Stableford, 1949; Gillespie, 1983) stimulates motility of their inner, basal ends. Isolated bottle cells cultured on glass in alkaline medium attach, spread and migrate on the substratum by their basal ends, whereas their apical ends are nonadhesive and remain inactive

(figs 7, 8, Holtfreter, 1944). Likewise, when explanted onto a substratum of endoderm, bottle cells form a pit reminiscent of the archenteron (fig. 16, Holtfreter, 1944). If bottle cells were to behave in this way *in vivo*, it was thought that they would drag surrounding tissues along with them, due to the firm association of surface cells in what Holtfreter (1943*a,b*) believed to be a syncytial ‘surface coat’.

Bottle cells could also act through their change in shape, rather than their invasiveness, by bending the sheet of cells to form a true invagination as their apices contract (see Baker, 1965). Lewis (1947), formalized the relation between cell shape and bending of the cell sheet to form an invagination with a mechanical model, made of rubber and brass. Odell and others did the same by computer simulation of cell shape changes (Odell *et al.* 1981; Hilfer & Hilfer,

1983). The relation of cell shape to bending of epithelial sheets has been reviewed in a number of publications (Gustafson & Wolpert, 1967; Schroeder, 1970; Burnside, 1973; Karfunkel, 1974; Schoenwolf, 1982; Ettensohn, 1985).

Several old observations and more recent experimental evidence suggest that amphibian bottle cells may have a more limited role, or perhaps a role different from those described above. Bottle cells disappear before the archenteron ceases to increase in depth (see Keller, 1986). Surgical extirpation of bottle cells in *Xenopus* results only in truncation of the peripheral archenteron (Keller, 1981; see also Cooke, 1975), which is the area to which they normally give rise (Keller, 1975). Moreover, most of the depth of the archenteron forms by involution instead of the invagination associated with bottle cell formation (Keller, 1986). Finally, the prospective fates and behaviour of bottle cells in the Mexican axolotl (Lundmark, 1986) and other urodeles (Holtfreter, 1944) are different from their counterparts in *Xenopus* (Keller, 1986). Looking at other systems, the careful studies of Ettensohn (1984) on primary invagination of the sea urchin revealed no clear relationship between cell shape and invagination of the vegetal plate. Likewise, extensive analysis of avian neurulation suggests that the relation of cell shape change to invagination and the mechanisms of such shape change may be more complex than previously thought (see Schoenwolf, 1985; Smith & Schoenwolf, 1987). The same applies to lens formation (Zwaan & Pearce, 1971; Hendrix & Zwaan, 1974).

Using several methods, we will show that the unique shape of bottle cells and their function in *Xenopus laevis* are not intrinsic to these cells but are dependent on a simple intrinsic behaviour, apical constriction, acting in a specific mechanical and geometrical context. In this context, apical constriction has the limited but perhaps important function of initiating the involution of the deep, leading edge of the involuting marginal zone (IMZ) prior to its convergence and extension later in gastrulation.

Materials and methods

Obtaining embryos, culture methods, cell marking

Xenopus laevis embryos were obtained by standard methods and dejellied chemically (0.6 g Tris, 1.75 g cysteine hydrochloride, in 50 ml distilled water adjusted to pH 7.8). Vitelline envelopes were removed manually with sharpened watchmaker's forceps (Dumont no. 5). Embryos were cultured in modified Niu-Twitty solution (buffered at pH 7.4 with 5 mM-Hepes) or in Danilchik's solution (Keller *et al.* 1985a,b). Microsurgery was done on a Plasticine base

(Harbutt's Plasticine Limited, Bath, England) with eyebrow hairs and hair loops. For tracing of cell fates, embryos were injected with fluorescein dextran amine (FDA) cell lineage tracer, obtained from Robert Gimlich (see Gimlich & Cooke, 1984), at the 1-cell stage, and the appropriate regions of labelled embryos were grafted homotypically to unlabelled embryos, using eyebrow hairs. To generate cuts of uniform, repeatable character for tissue gaping studies, an electric, vibrating microknife (60 cycles s^{-1}) of tungsten developed for microsurgery in this laboratory by Chris Luzzio, was used. The developing embryos were fixed in 4% formaldehyde at the appropriate stage, embedded in Paraplast, sectioned at 10 μm and the labelled cells visualized by epifluorescence microscopy. Staging was according to Nieuwkoop & Faber (1967).

Cinemicrography, videomicrography, SEM and morphometrics

Cinemicrography was done with a Bolex-Sage or Arriflex camera and intervalometer, using Kodak Plus X reversal or Ektachrome Video-news film. Videomicrography was done with a Panasonic recorder, camera and monitor. A Zeiss Standard microscope and low-angle epi-illumination were used throughout. The shapes of the apices of the forming bottle cells and of the adjacent marginal zone and vegetal cells were determined by tracing cell profiles with a Numonics digitizer, supplemented by an Apple II+ computer and a morphometrics program written for this laboratory by Chet Regen. The morphometric parameters will be described in the Results.

Simulation of bottle cell function with an axisymmetric finite element program

In order to determine what effect specific bottle cell behaviours could be expected to have on surrounding tissues, we used an axisymmetric finite element formulation developed by Louis Cheng (see Hardin & Cheng, 1986). Briefly, the formulation models the stretching, bending and shearing of rotationally symmetric shell-like bodies. The shape of the embryo is specified by a meridian curve rotated about the axis of symmetry to yield a three-dimensional shape. The deformation of this model embryo under the influence of various forces can be simulated using a computer algorithm described elsewhere (Cheng, 1987a). Bottle cells do form symmetrically about the animal-vegetal axis, although not all at the same time. *In vivo*, the process begins dorsally in late stage 9, proceeds laterally and is completed ventrally by stage 10.5. Since the process of bottle cell formation and the associated deformation of the embryo do not appear to differ around the blastopore, we idealize bottle cell formation as occurring simultaneously in all sectors.

Results

Normal bottle cell formation

The prospective bottle cells form from the six to eight tiers of superficial epithelial cells that lie at the vegetal end of the involuting marginal zone (IMZ)

and immediately animal to the much larger epithelial cells that comprise the vegetal region (Fig. 1). The earliest stages of their formation are characterized by apices that (1) are smaller in area than the surrounding IMZ cells; (2) have a higher density of microvilli on their apices (Figs 1, 2A) and (3) appear grey by virtue of increased apical pigment concentration (Fig. 2A). The first bottle cells to form are not necessarily neighbours nor are groups necessarily contiguous (Fig. 1). Their apices are pleiomorphic and most lack obvious major and minor axes (Figs 1, 2A). The sagittal profile of the bottle cell area is deformed very little at this early stage (Fig. 2A). As bottle cell formation proceeds, their apices darken, form a larger, more contiguous array and acquire an elongate shape with their long axes coming to lie parallel to the circumference of the mass of large cells at the vegetal pole (Fig. 2B). During this period, the

bottle cell region bends and the blastoporal groove forms along bottle cells, accompanied by the outward bulging of the IMZ above the groove (Fig. 2B). Subsequently, the constricted apices of the bottle cells join to form the blastoporal pigment line characteristic of the stage 10 or 10+ embryo (Nieuwkoop & Faber, 1967); (Fig. 2C). The apices become highly elongate and aligned, and the bottle cell region invaginates to form the blastoporal groove (Fig. 2C). Early forming bottle cells tend to lie in clumps and have more isomorphic apices than those forming later, which have very elongate apices (Fig. 3A–C). As bottle cells form, the IMZ cells immediately above them become elongate in the animal–vegetal direction whereas those at greater distances remain rounded (Fig. 3D). The same is true of the vegetal cells adjacent to the bottle cells (Fig. 3D). Bottle cell formation progresses laterally and finally ventrally,

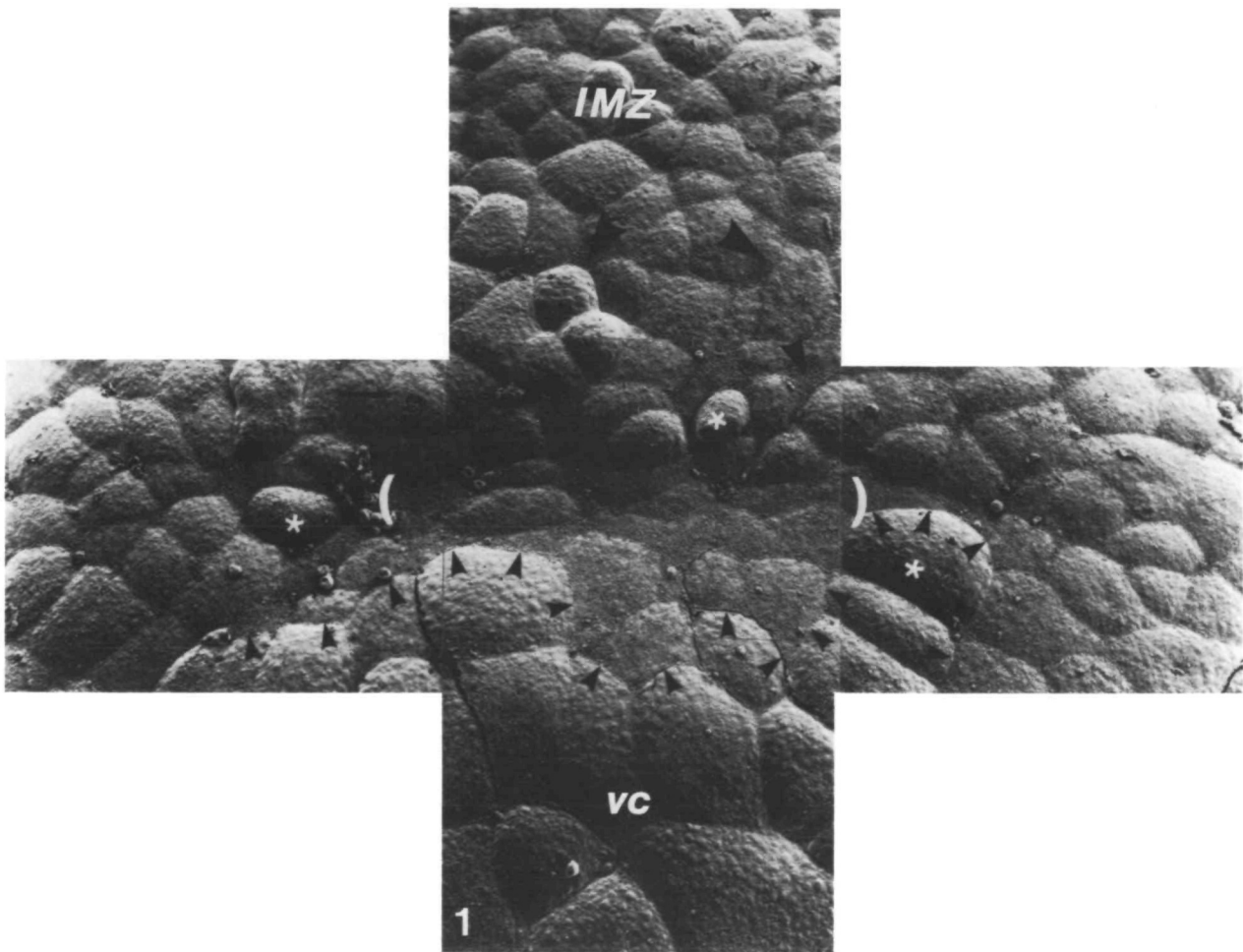
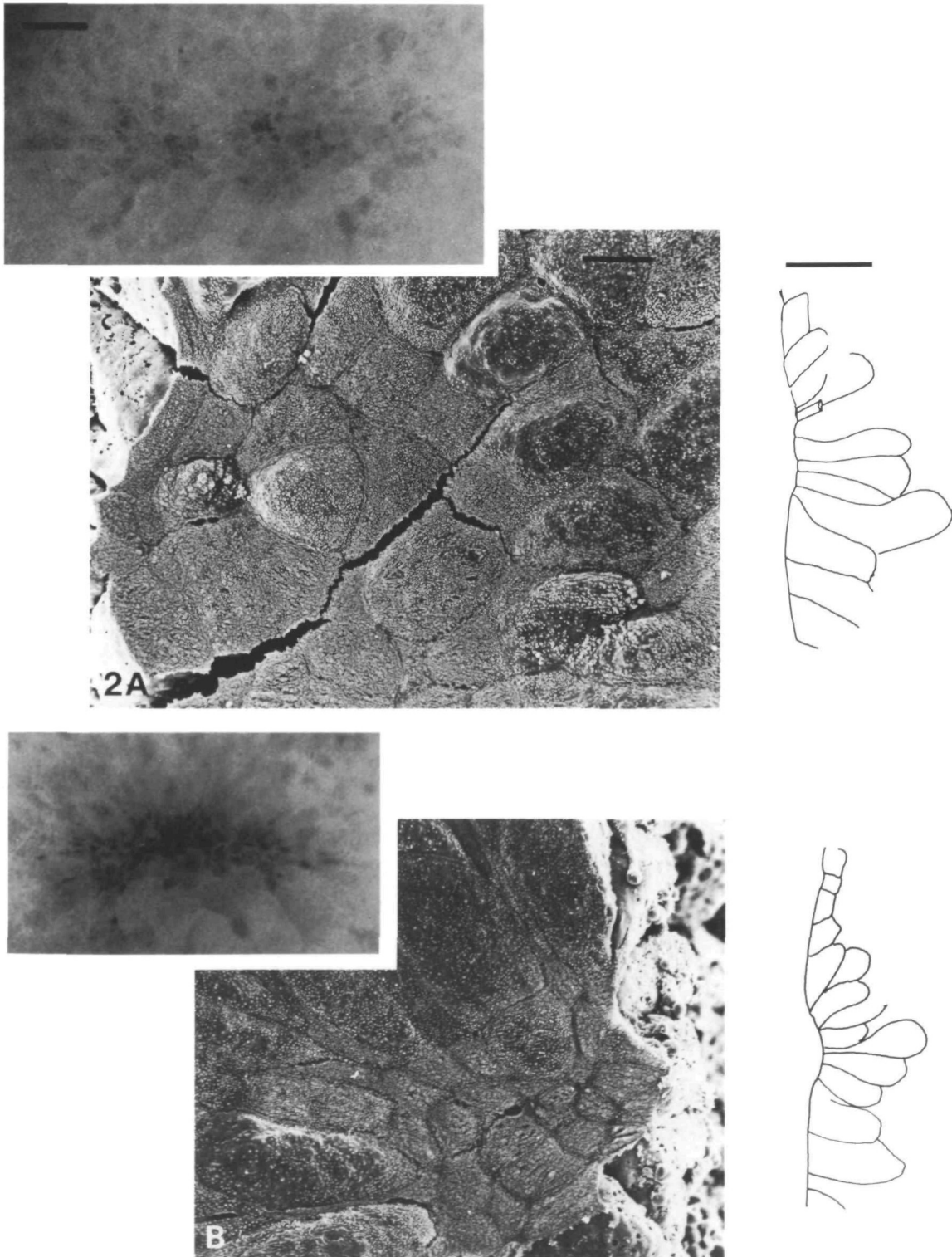


Fig. 1. A scanning electron micrograph of an early stage of bottle cell formation in *Xenopus laevis* shows the forming bottle cells, characterized by larger numbers of microvilli on their apical surfaces. The main population of bottle cells lies between the white brackets and its boundary with the large vegetal cells (*vc*) is outlined by small pointers. More bottle cells form from the involuting marginal zone (*IMZ*) epithelial cells. Some form near or adjacent to the main population (medium pointers) and some form four or five tiers of cells above the main population (large pointers). Some cells fail to participate in bottle cell formation (asterisks) although they are surrounded or nearly surrounded by bottle cells. Magnification: $\times 294$. Bar, $25\ \mu\text{m}$.

surrounding the vegetal cells (the yolk plug) in a manner indistinguishable from what has been described for the dorsal region.

Time-lapse micrography shows that, as their apices contract, the prospective dorsal bottle cells move vegetally, against the boundary of the large vegetal cells, to form the blastoporal pigment line (BPL) (Fig. 4A,B). The dorsal marginal zone cells lying at

or just beyond the edge of the prospective bottle cell region move some distance toward the BPL whereas the corresponding vegetal cells move less or not at all (Fig. 4C). As the prospective bottle cell region contracts into the BPL in lateral and ventral sectors, both the animal boundary (filled circles, Fig. 4D) and vegetal boundary (filled squares, Fig. 4D) of the prospective bottle cell region move vegetally



(Fig. 4E,F) and appear to constrict the vegetal cell mass. Note that the large area originally occupied by the prospective bottle cells (shaded areas, Fig. 4A,D) disappears into the BPL by stage 10.5 (Fig. 4E,F) and the vegetal cell mass is decreased in area by about 30% at the end of bottle cell formation (Fig. 4E,F).

Quantitative analysis of changes in cell shape among bottle cells and adjacent tissues

Quantitative analysis of the shape changes of bottle cells and adjacent cells under normal and experimental conditions clarifies the cellular mechanics of bottle cell function. Two morphometric parameters are relevant. First, the length–width ratio of individual cells (l/w). This is the length of the longest line that

can be placed within the cell divided by the profile of the cell projected onto a line perpendicular to the long axis (Fig. 5, top panel). The second is the profile of the cell projected onto the animal–vegetal meridian of the embryo divided by the profile projected onto a latitude line perpendicular to the animal–vegetal meridians (y/x) (Fig. 5, bottom panel). The former is a measure of the elongation of the apices of the cells and the latter is a measure of the orientation of any cell that shows significant elongation. Changes in these parameters summarize change in shape of the bottle cell apices (Fig. 5). As bottle cell apices contract, they become elongate in shape (mean l/w rises from 1.6 to over 4) and align parallel to their boundary with the large vegetal cells (y/x falls from

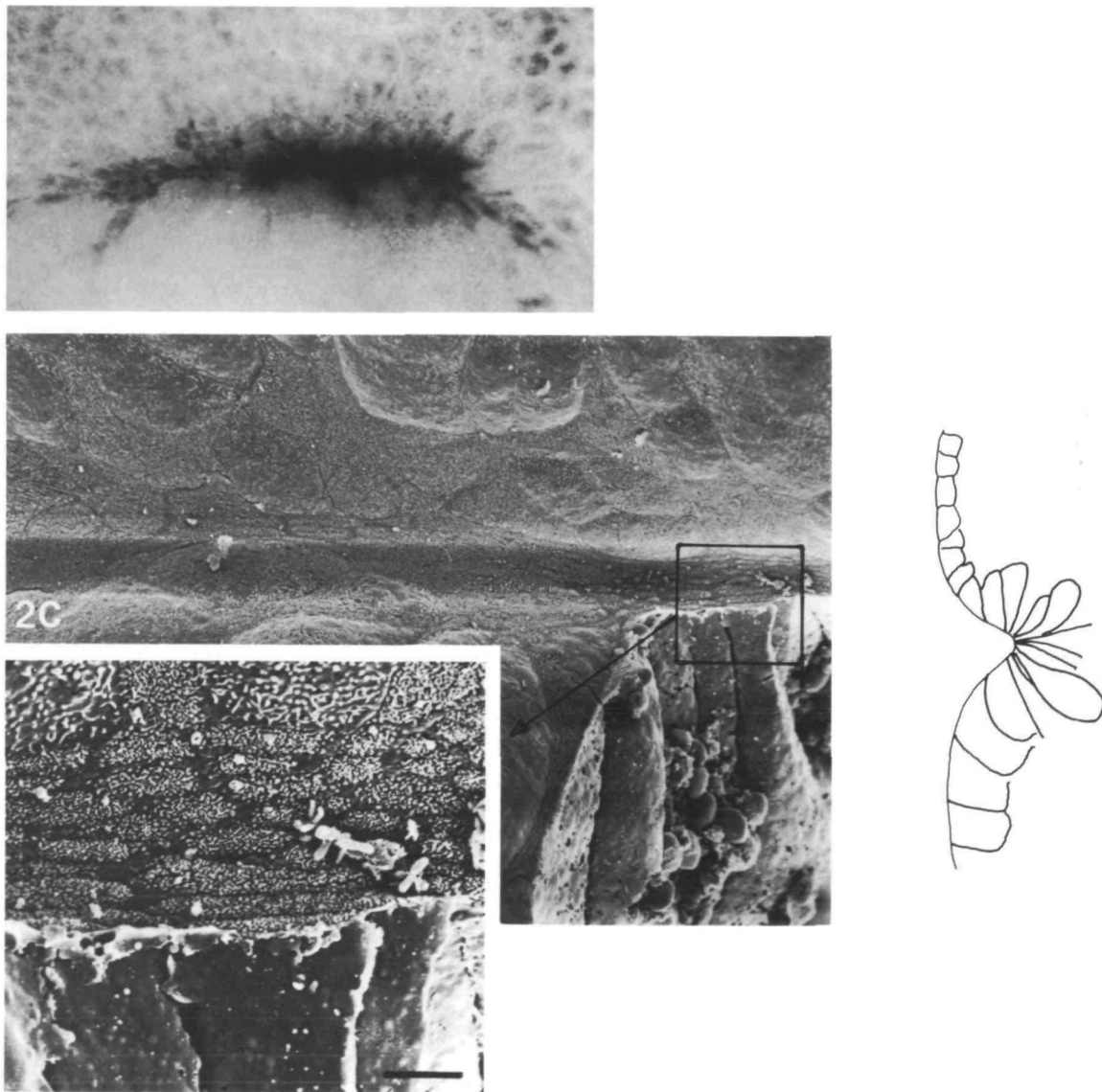


Fig. 2. The early (A), middle (B) and late (C) stages of bottle cell formation are illustrated by light microscopy of their apical surfaces (upper left insets), scanning electron micrography of the apical surfaces (centre) and sagittal profiles (right) of the bottle cell region at each stage. Magnification: light micrographs, $\times 100$, bar, $100\ \mu\text{m}$; SEMs, $\times 550$, bar, $20\ \mu\text{m}$; SEM inset in C, $\times 2100$, bar, $5\ \mu\text{m}$; profiles, $\times 135$, bar, $100\ \mu\text{m}$.

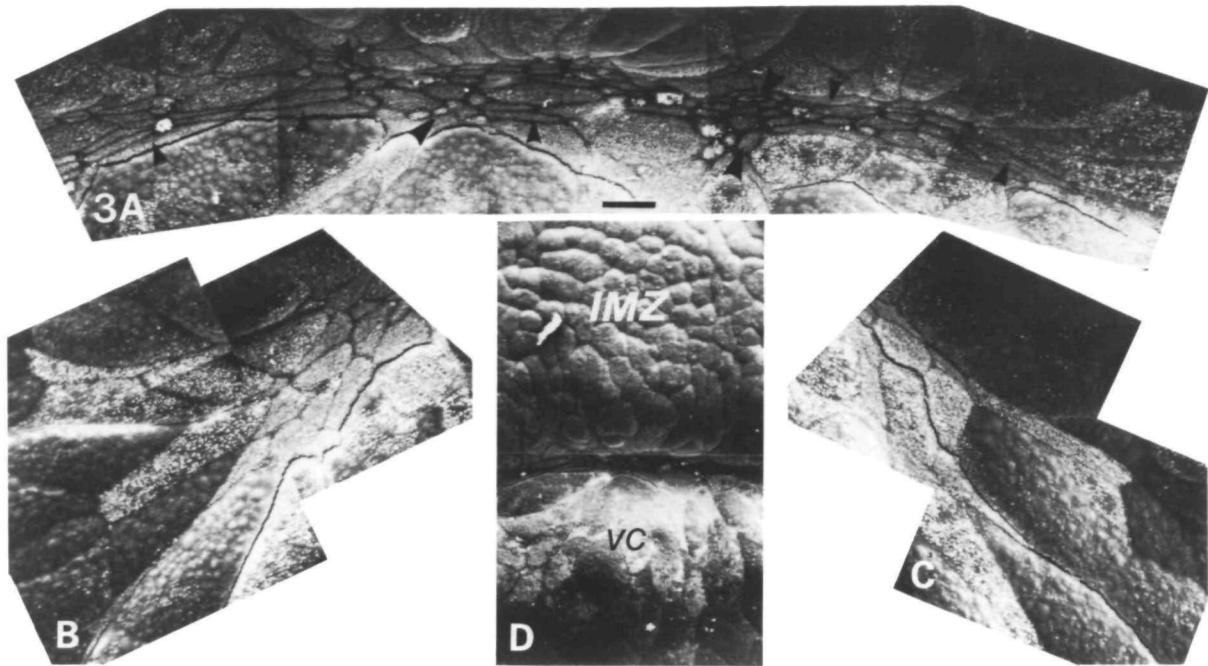


Fig. 3. The late stage of dorsal bottle cell formation is illustrated by SEMs of the centre (A), left end (B) and right end (C) of the blastoporal pigment line at stage 10. The morphology of the apices of cells in the adjacent involuting marginal zone (IMZ) and vegetal cells (vc) are also shown (D). Magnification: A–C, $\times 250$, bar, $20\ \mu\text{m}$; D, $\times 90$.

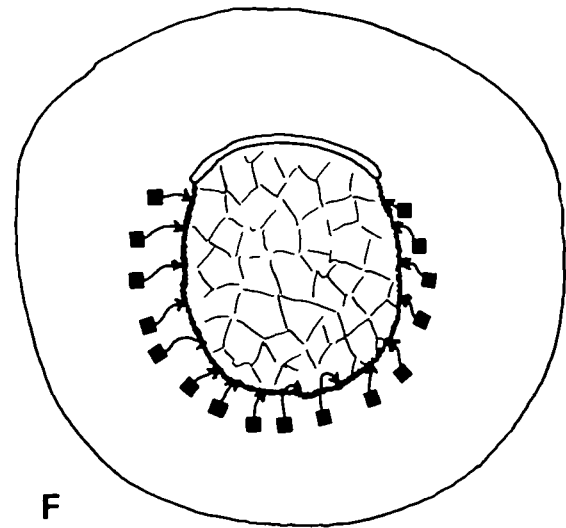
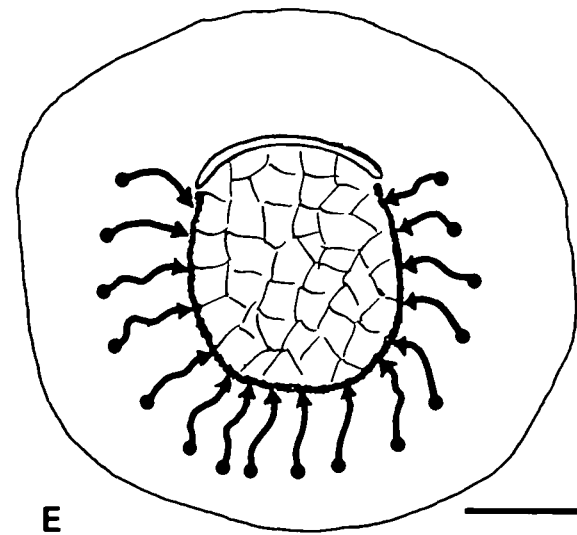
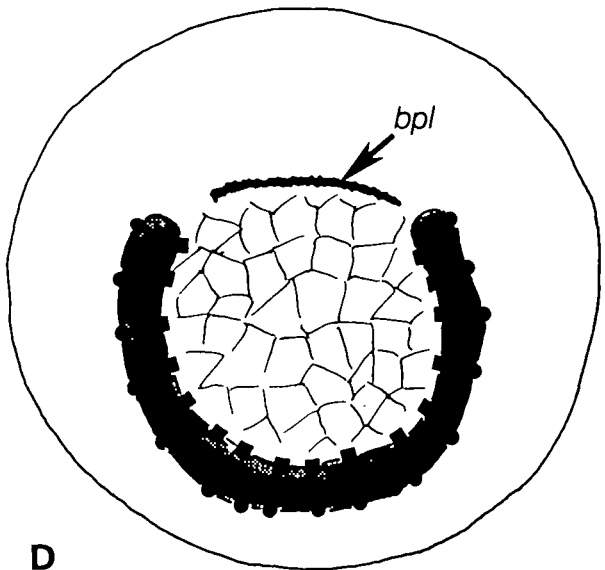
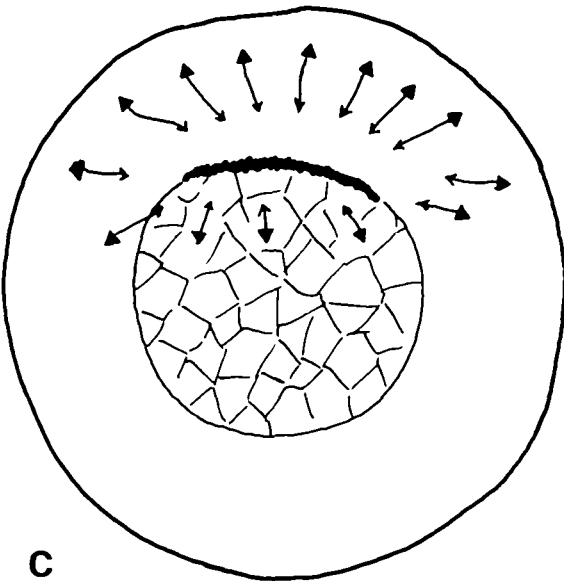
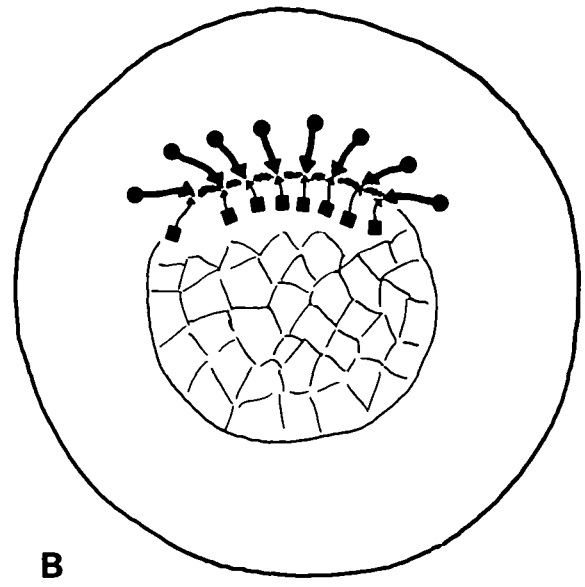
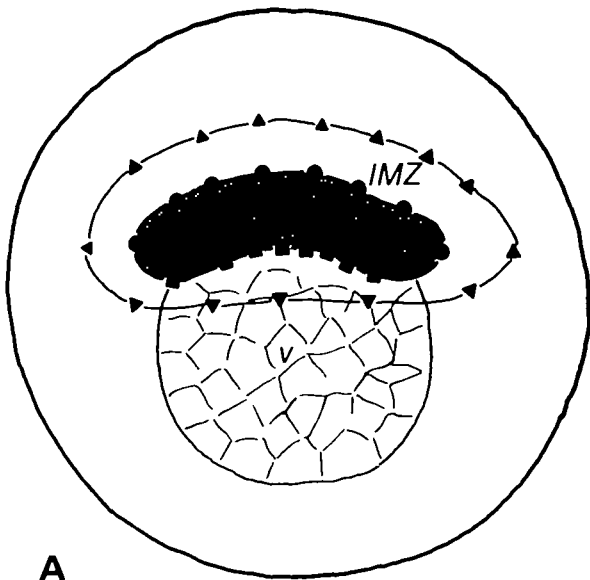
0.9 to 0.4). At the same time, the IMZ cells above the bottle cells become elongate (mean l/w changes from 1.4 to 1.9) and align perpendicular to the long axes of the bottle cell apices (y/x rises from 0.9 to 1.7). To a lesser extent, the vegetal cells below the bottle cells do the same (Fig. 3D; Fig. 5).

Comparison of bottle cell behaviour with and without adjacent tissues

Is the development of the characteristic apical shape and the directional, vegetal displacement of the forming bottle cells autonomous to these cells or is the anisotropy imposed by neighbouring tissues on an intrinsically isotropic motile activity? Altering the relationship of bottle cells to the surrounding tissues shows that the latter is the case.

Apices of prospective bottle cells, which were excised from the dorsal side at stage 9 and cultured on a nonadhesive agarose substratum, contract uniformly, forming rounded apices (Fig. 6A–C) rather than the elongate ones found *in vivo* (Figs 2C, 3D). The mean length/width ratio in culture was 1.6 (s.e. = 0.05) compared to 4.2 (s.e. = 0.17) *in vivo* (Fig. 5). Moreover, the apical–basal elongation characteristic of bottle cells *in vivo* does not occur in culture (Fig. 6D). Instead, an unconstrained sheet of forming bottle cells bends to form a cup that nearly closes at the open end, with the basal ends of the nearly spherical cells forming its outer surface (see Fig. 12A). This suggests that bottle cells have an

Fig. 4. These diagrams are vegetal views of an embryo during bottle cell formation, showing tracings of cell movements recorded by time-lapse methods. The dorsal side is above in all illustrations. Using time-lapse recording, the prospective dorsal bottle cell area was mapped, retrospectively, onto the stage-9 embryo (shaded area, A). The margin of the prospective bottle cell area lying in the involuting marginal zone (IMZ) is indicated by filled circles; the vegetal boundary is indicated by filled squares. During bottle cell formation, the margins of this area move into the blastoporal pigment line of the stage 10+ early gastrula (arrows associated with circles and squares, B). Cells lying some distance away from the bottle cell region also move during this period (arrows associated with triangles, C). The area of the remaining prospective bottle cells, those of the lateral and ventral sectors, is mapped retrospectively on to the stage 10+ early gastrula (shaded area, D). The boundary of this area in the IMZ is indicated by filled circles and its vegetal boundary is indicated by filled squares. The movements of the IMZ boundary into the blastoporal pigment line (*bpl*) of stage 10.5 is shown (arrows, E). The movements of the vegetal boundary into the blastoporal pigment line is also shown on a diagram of the same embryo (arrows, F). The darkly shaded patch in the prospective bottle cell region of A shows where patches of labelled bottle cells or bottle cells and underlying deep cells were grafted into unlabelled embryos to produce the results in Fig. 14D–G. Bar, $0.5\ \mu\text{m}$.



autonomous tendency to contract uniformly and that the anisotropic contraction and apical-basal elongation seen *in vivo* are results of the mechanical constraints imposed by surrounding tissues. A reasonable hypothesis is that the large mass of vegetal cells cannot be displaced or deformed, thus constraining the bottle cells to contract in the animal-vegetal

direction and resulting in a ring of elongate apices surrounding the vegetal cells.

To test this notion, we removed a large fraction of the vegetal cells of the late blastula immediately before bottle cell formation had begun by sucking them out with a fine micropipette. Under these conditions, the bottle cell apices are much less

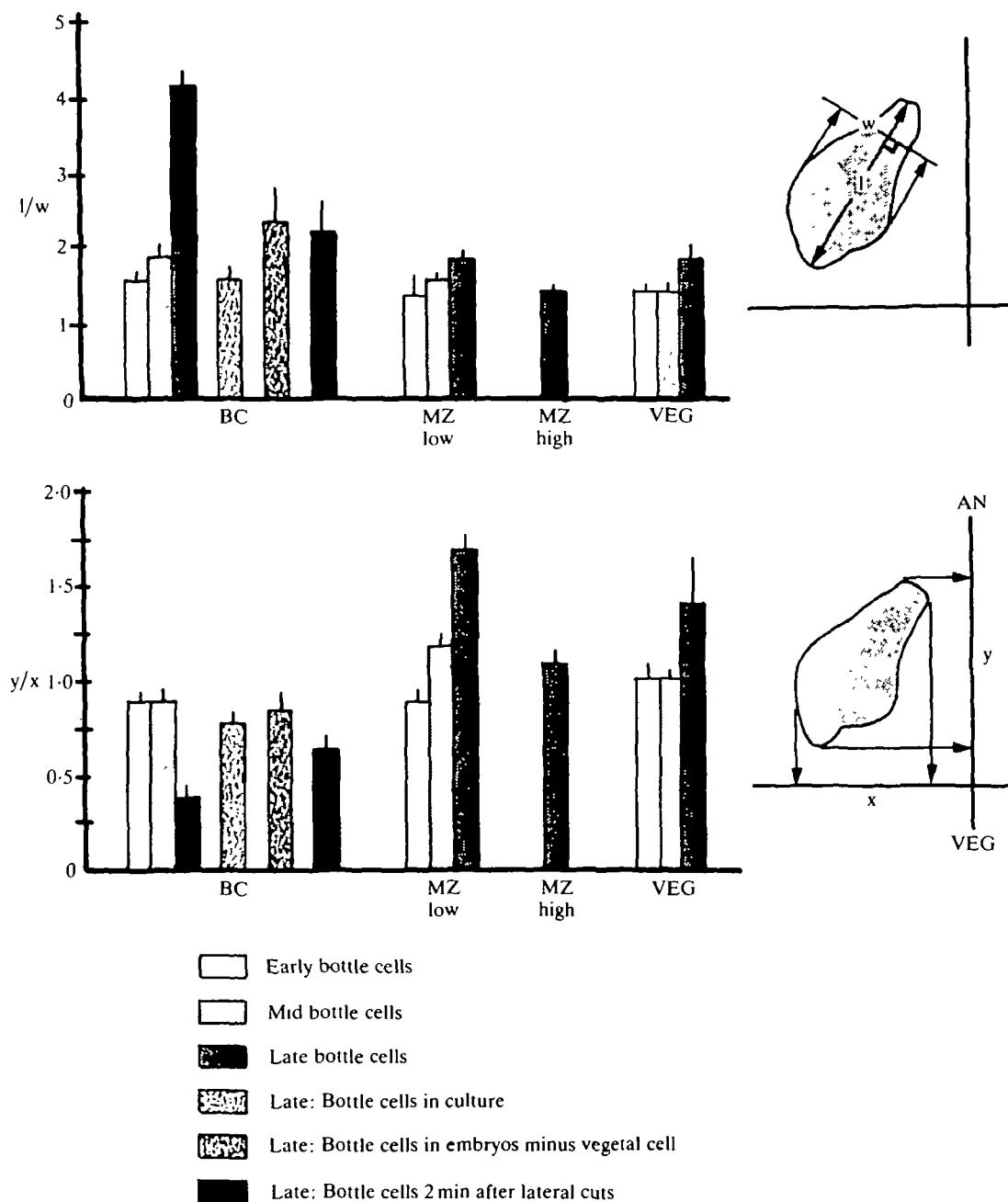


Fig. 5. The mean length width ratios (l/w , above) and the mean projected length width ratios (y/x , below) of bottle cells (BC), marginal zone cells (MZ), and vegetal cells (VEG) are shown for early, middle and late stages of bottle cell formation, and for late bottle cells under three different experimental conditions described in more detail in the text. The low marginal zone includes the first four tiers of cells above the bottle cell region; the high marginal zone includes rows 7 through 11. The standard error of the mean is indicated at the top of each bar and the numbers above the bars indicate the number of measurements, which were the same for l/w and y/x .

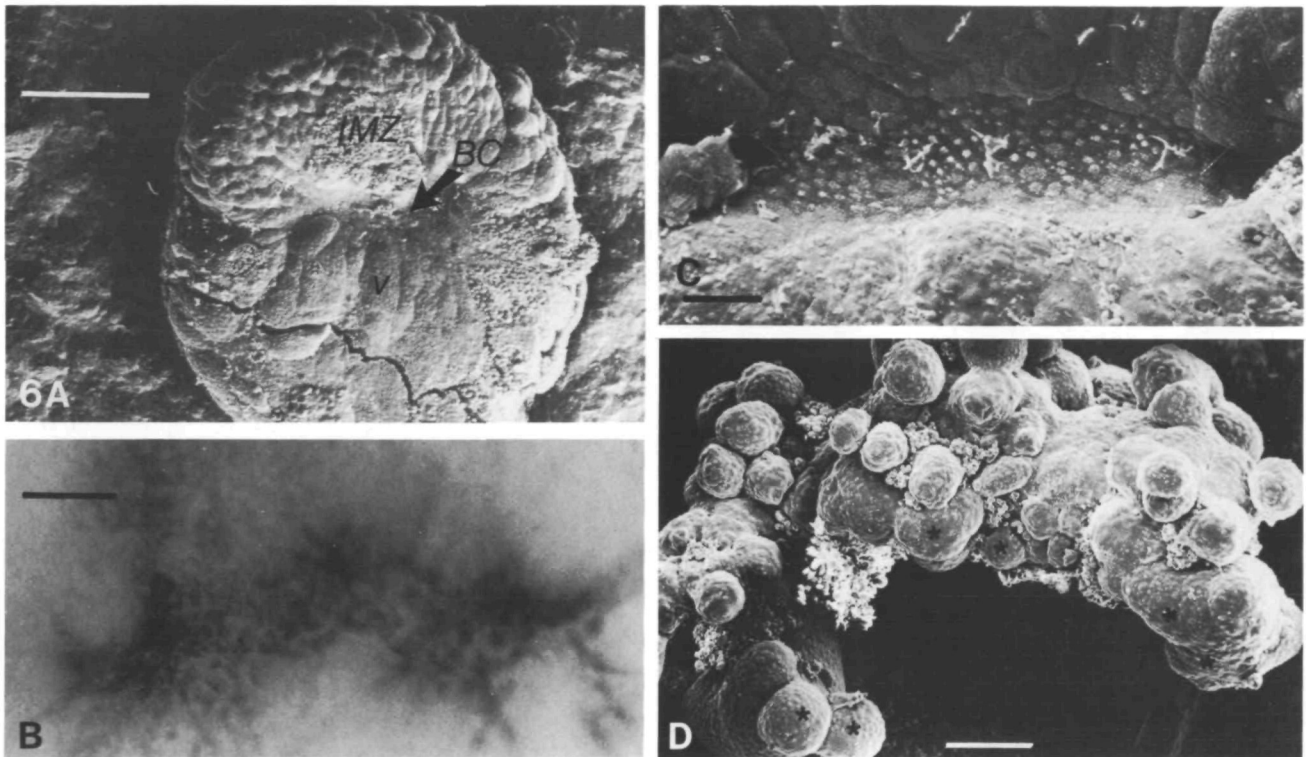


Fig. 6. An SEM shows a bottle cell region (*BC*) that formed in a region of the dorsal sector of a late blastula excised and cultured on a nonadhesive agarose substratum (*A*). The marginal zone (*IMZ*) and vegetal region (*v*) are indicated. A light micrograph shows the rounded, pigmented apices of the bottle cells in the specimen above (*B*). An SEM shows the uniformly rounded apices of bottle cells formed in cultured explants (*C*). An SEM of an isolated bottle cell region showing 'bottle' cells (asterisks) radiating from the blastoporal pigment line lying hidden on the bottom (concave) side of the explant (*D*). Magnification: *A*, $\times 70$, bar, $0.2\ \mu\text{m}$; *B*, $\times 190$, bar, $50\ \mu\text{m}$; *C*, $\times 345$, bar, $25\ \mu\text{m}$; *D*, $\times 135$, bar, $50\ \mu\text{m}$.

elongate (mean $l/w = 2.4$; s.e. = 0.15) and less aligned ($y/x = 1.8$; s.e. = 0.15) (Fig. 7*A,B*) than those in normal embryos (Fig. 5). In these respects, they resemble bottle cells forming in culture rather than those forming *in vivo*.

These results again argue that the anisotropic contraction of bottle cells reflects an anisotropic environment, specifically, the large mass of vegetal cells on one side and the *IMZ* on the other. Moreover, these results argue that the isotropy in cultured bottle cells is due to the absence of the large mass of vegetal cells that normally offer resistance to contraction in the circumferential direction. In these embryos, there are many more bottle cells relative to the circumference they enclose and the hoop-stress normally found encircling the mass of vegetal cells never develops.

If circumferential contraction of bottle cells is resisted by the vegetal cell mass in normal embryos, bottle cells should contract rapidly and lose their circumferential elongation when cut free along animal-vegetal meridians. This is the case. If the bottle cell region is cut free from the embryo on all sides, it contracts in all directions, but particularly in the circumferential direction (Fig. 8), and within 2 min after lateral excision from adjacent tissues, the elongate shape and circumferential orientation of the bottle cell apices decrease dramatically (Fig. 5).

Displacement of the IMZ vegetally during bottle cell formation

This evidence suggests that bottle cells contract in all directions but their position as a ring adjacent to the large mass of vegetal cells constrains them to shorten

primarily in the animal-vegetal direction, displacing the IMZ vegetally rather than moving the vegetal region animally. Thus the IMZ epithelium is easier to deform than the vegetal epithelium, either because the latter are more rigid or because of their position at one pole of the embryo.

However, the mechanical effect of bottle cell formation on the IMZ seems confined to about six or seven tiers of cells above the bottle cells. The

elongation and alignment of IMZ cells decreases with distance from the bottle cells. Beyond six or seven cell diameters, no effect is apparent and even late in bottle cell formation the apices of cells in the upper IMZ are not significantly different from IMZ cells before bottle cell formation (MZ, high, Fig. 5). The greater distortion of cell apices near the bottle cells reflects greater tension there. To estimate the tension in the epithelial sheet, wounds of identical width and

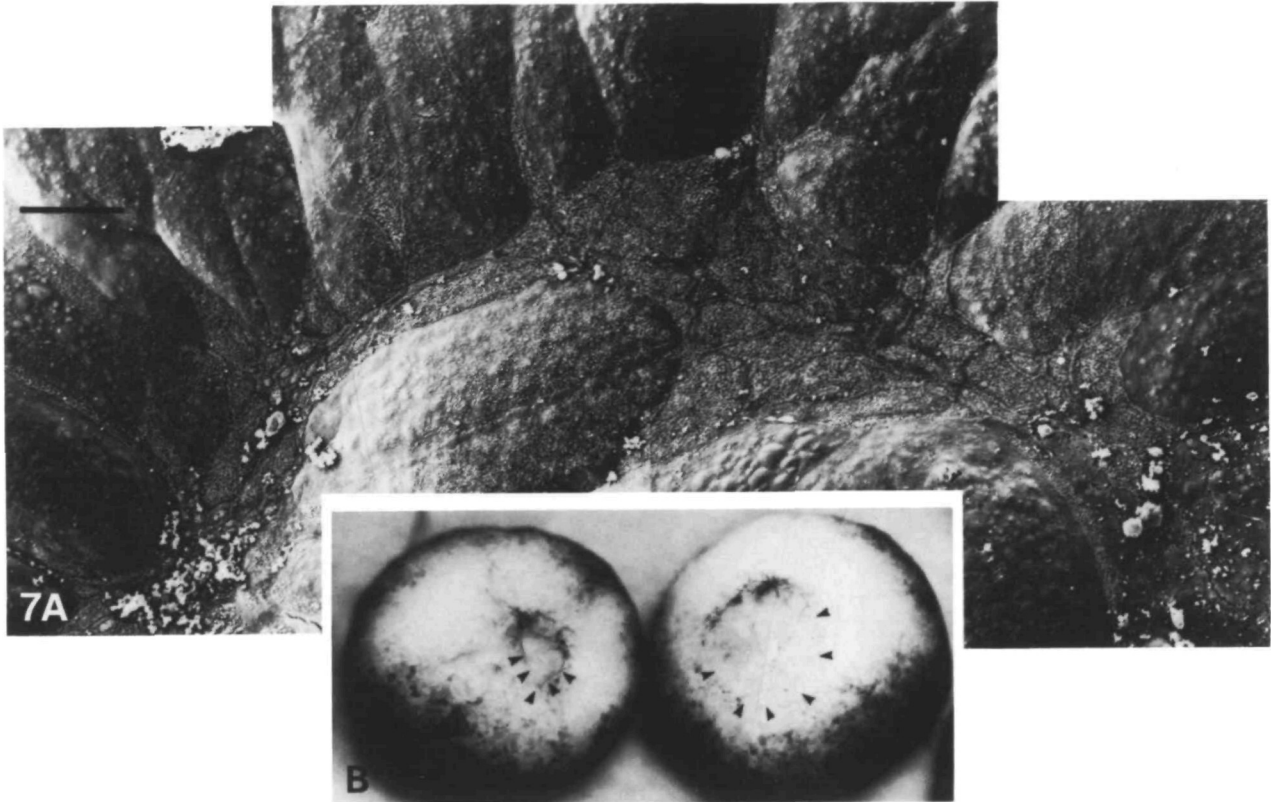


Fig. 7. An SEM shows apices of bottle formed in embryos from which most of the vegetal cells have been removed (A). Light micrographs (B) show the site of bottle cell formation as indicated by the blastoporal pigment line in this embryo (left) and a control (right) embryo at stage 10. The vegetal cell mass in both is outlined with small pointers. Magnification: A, $\times 850$, bar, $25\ \mu\text{m}$; B, $\times 38$.

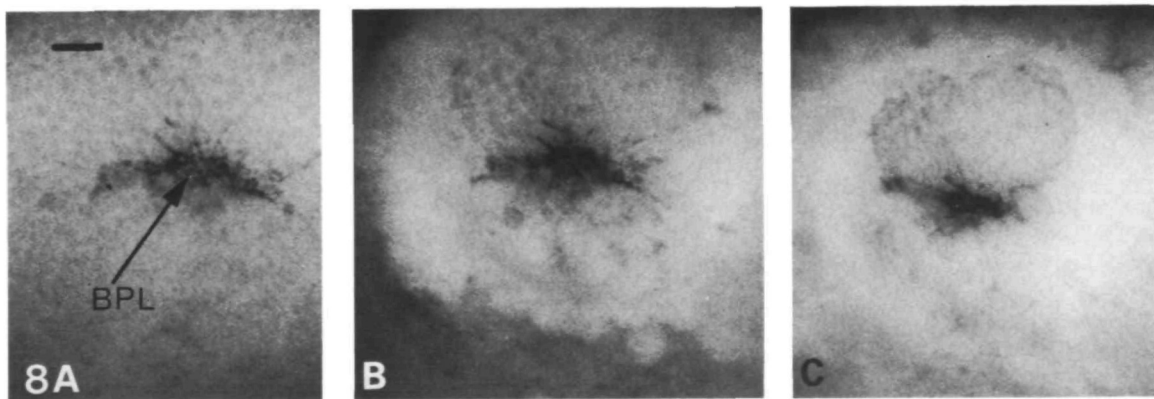


Fig. 8. Light micrographs show the bottle cell region (blastoporal pigment line, BPL) of an embryo at stage 10 (A), 30 s (B) and 4 min (C) after all lateral connections of the bottle cell region to the surrounding tissue were cut. Magnification: $\times 59$, bar, 0.1 mm.

depth were made with the vibrating tungsten micro-knife immediately above the bottle cells and at increasing distances toward the animal pole. The embryos were fixed 30 s after wounding and the gape of the wounds measured. The mean gape is $300\ \mu\text{m}$ (± 80 s.d.) just above the bottle cells but decreases to $105\ \mu\text{m}$ ($\pm 23\ \mu\text{m}$ s.d.) at nine to twelve tiers of cells away (Fig. 9A,C), beyond which there is no further decrease. This, and the shapes of IMZ cells described above, suggest that the mechanical influence of bottle cell formation is confined to six or seven tiers of cells from the bottle cells. However, the tension in the first or second tier of IMZ cells is great and is perhaps near the normal limits of intercellular adhesion; a common defect among laboratory-reared *Xenopus* is tearing of the epithelium in this region.

Bending of the IMZ during bottle cell formation

The deformation of the sagittal profile of the embryo is not the same above and below the forming bottle cells (Fig. 10A). The IMZ typically bends outward (Fig. 10B) whereas the vegetal region moves directly inward (Fig. 10C). The latter movement is probably due to the hoop stress described above. The bending of the IMZ is due, in large measure, to the fact the basal ends remain large and the apical half of the cells narrow and elongate to form gradually tapered necks as the apical contraction occurs (Fig. 2). Apical contraction is probably an active event and the apical-basal elongation a passive one resulting from the fact that the IMZ resists the outward bending demanded by the apical contraction. If the epithelium is cut just above the bottle cells, the bottle cells immediately rotate vegetally over their own apices, turn their basal ends outward and, in the process, shorten and lose their bottle shape within 30 s (Fig. 9A). Similar behaviour occurs when the cut is made immediately vegetal to the bottle cells (Fig. 9B). Such behaviour is not observed in the adjacent marginal zone, whether the cut is made close to or far from the bottle cell array (Fig. 9C). Moreover, in cultured explants, where there is little surrounding tissue to resist bending, the 'bottle' cells do not show apical-basal elongation and develop short, steeply tapered necks instead of long gradually tapered ones following apical contraction. These facts suggest that the apical-basal elongation and the 'bottle' shape is the product of an intrinsic apical constriction interacting with the external mechanical environment.

Finite element simulation of bottle cell effects on surrounding tissue

A reasonable hypothesis from these results is that bottle cells show only one intrinsic motile behaviour

during their formation, i.e. apical constriction. Because they lie at the edge of a large mass of vegetal cells that does not deform easily, their apical contraction is largely accommodated by vegetal movement of the IMZ and the squeezing of their cell bodies basally rotates the IMZ outward. Whether or not this could produce the observed distortion of the embryo depends on the mechanical and geometric properties of the adjacent tissues. In order to test these notions and to define which properties of adjacent tissues might be important, we have simulated the mechanics of bottle cell formation using Cheng's finite element algorithm (see Hardin & Cheng, 1986). This method has already been used to model the deformation of sea urchin eggs (Cheng, 1987b) and the response of the sea urchin gastrula to filopodial pulling by secondary mesenchyme cells (Hardin & Cheng, 1986).

We imposed a bending moment analogous to the isotropic contraction of the bottle cells observed in culture over three elements of the fifty elements comprising the entire animal-vegetal meridian. We also varied the animal-vegetal position of the three-element bottle cell region, the thickness of the adjacent IMZ and vegetal cell mass and the stiffness of these two regions. Because the method requires that the thickness of the shell being simulated should not exceed a fifth of the radius, we could not do simulations using the full thickness of the vegetal region, which is nearly equal to the radius of the embryo. This does not appear to be a problem, however. The central core of endodermal cells appears to be homogeneous throughout the region affected by bottle cell formation, forming a homogeneous background on which the variation in the superficial epithelium is superimposed. If the central endodermal cells of the vegetal region are removed through the blastocoel roof by a suction pipette, the effect of bottle cell formation and the subsequent gastrulation appears normal (data not shown). Moreover, the simulations themselves suggest that vegetal thickness of the order of the epithelial layer is appropriate to produce the proper morphogenesis.

A near perfect mimic of the normal deformation in the bottle cell region was achieved with a simulation in which the animal cap, IMZ and vegetal region were graded in thickness, as *in vivo*, and the stiffness was equal in all regions (Fig. 11A). Doubling the stiffness of the vegetal region results in more dramatic rolling of the IMZ outward and less inward movement of the vegetal region (Fig. 11B). Equal thickness and stiffness in all regions results in a greater and more local indentation of the vegetal region and less rolling of the IMZ (Fig. 11C). If the position of the bottle cells is moved nearer the equator, there is less rolling of the marginal zone outward relative to squeezing of the endoderm inward (Fig. 11D). This situation is

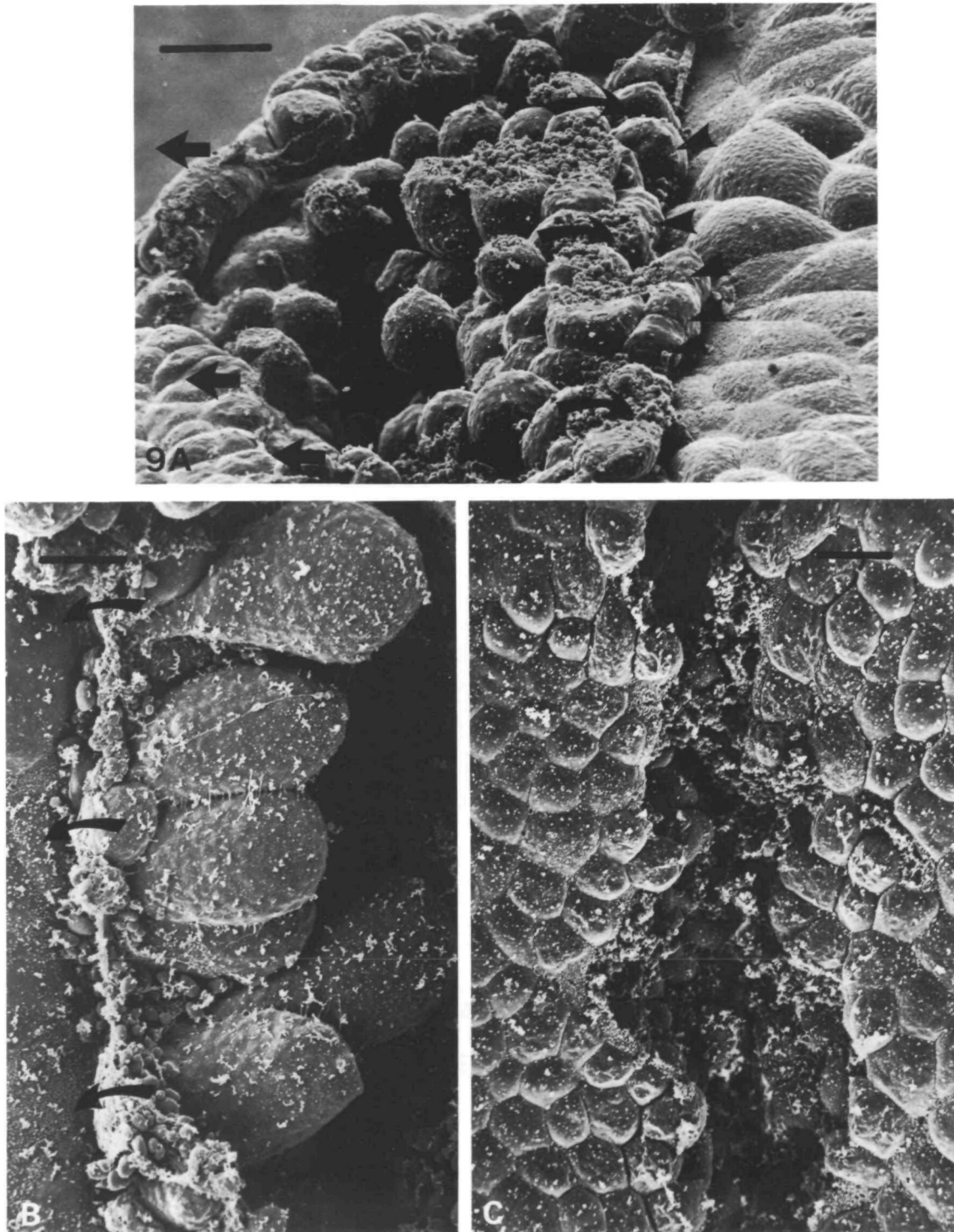


Fig. 9. An SEM of a specimen fixed 30 seconds after cutting through the epithelial cells immediately above the bottle cells shows rotation of the bottle cells (pointers) vegetally (curved arrows) such that their basal ends are outermost and their apices are facing inward (A). The marginal zone retracts animalward some distance (straight arrows). A cut through the superficial epithelium immediately below the bottle cells results in rapid rotation of the bottle cells in the opposite direction (animalward, curved arrows) and rapid loss of the 'bottle' shape (B). The same wound 300 μm animal to the bottle cells produces no such rotation of cells at the wound margins (C). Magnifications: A, $\times 350$, bar, 50 μm ; B, $\times 530$, bar 25 μm ; C, $\times 450$, bar, 25 μm .

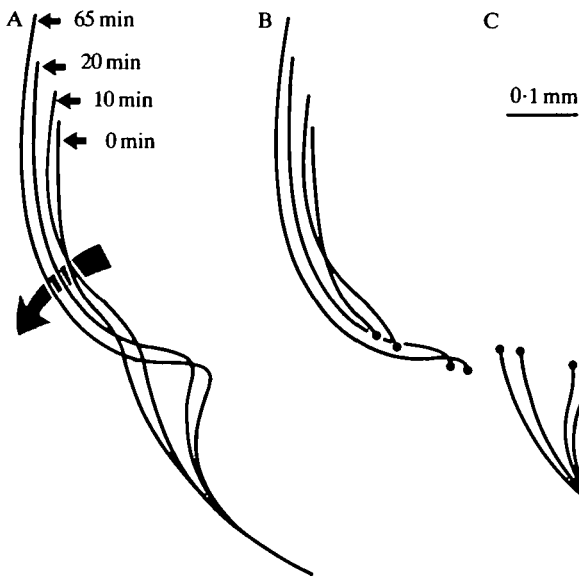


Fig. 10. Tracings from a time-lapse film show the changes in the sagittal profile of the bottle cell region, the marginal zone and the vegetal region during bottle cell formation. The deformation of all three regions is shown together in A. In B, the marginal zone, including the blastoporal pigment line and bottle cells, is shown. In C, the vegetal region, up to the lower edge of the blastoporal pigment line, is shown. Note rotation of the marginal zone outward (dark arrow) and movement of the vegetal region directly inward (light arrow). Magnification: $\times 250$, bar, 0.1 mm.

reminiscent of actual embryos in which bottle cell formation occurs abnormally high on the animal-vegetal axis: such embryos have large, protruding yolk plugs and fail to undergo involution properly (data not shown).

Bottle cell respraying in culture and in vivo

Prospective dorsal bottle cells explanted to culture constrict their apices to form a BPL (Fig. 12A; 0.5 h). They then form a pit lined at the bottom with the constricted apices of the bottle cells (Fig. 12A; 1.0 h). They remain in this configuration until controls reach stage 11, at which time they begin to expand and respread to cover a large area of the explant (Fig. 12A; 2-3.8 h). The cells moving out of these pits resemble a typical epithelium in the scanning electron microscope and are covered by irregularly distributed microvilli. The densities of microvilli and pigmentation fall as the bottle cells respread (Fig. 12B-C).

The corresponding cells at the anterior tip of the archenteron of control embryos show a similar decrease of pigmentation to speckled grey (Fig. 13A), respraying of their apices (Fig. 13B) and loss of microvilli (Fig. 13C). These results are consistent with previous work suggesting that bottle cells respread *in vivo* to form a large part of the epithelium

lining the periphery of the archenteron (Keller, 1981). To confirm that these cells are actually re-spread bottle cells, prospective dorsal bottle cells from FDA-labelled embryos were cut out and grafted

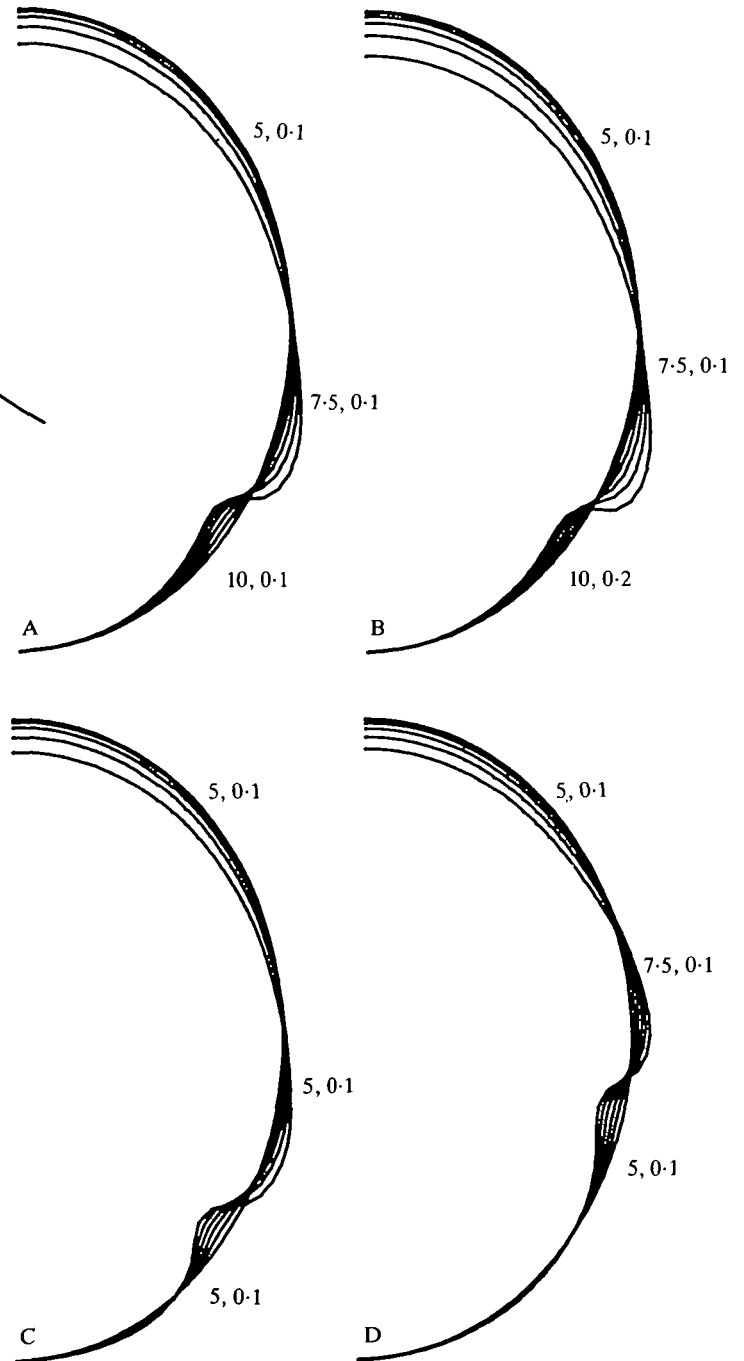


Fig. 11. Finite element simulations of bottle cell formation show change in shape of the embryonic profile under several conditions. Each profile represents 50 elements, numbered from the animal pole (top) to the vegetal pole (bottom). The bottle cells are located at elements 35-37 in A-C and at elements 28-30 in D. The thickness and the relative stiffness, in that order, are indicated for the animal region, the IMZ, and the vegetal region are also indicated.

into the corresponding region of an unlabelled host embryos at stage 9 (position of graft is shown in Fig. 4A). By the early gastrula stage, the grafted cells acquire the bottle shape (Fig. 13D) and, by the late

gastrula, they respread to form the anterior wall of the archenteron (Fig. 13E). They remain at this location and have been seen in the liver region as late as the tail bud stage (data not shown).

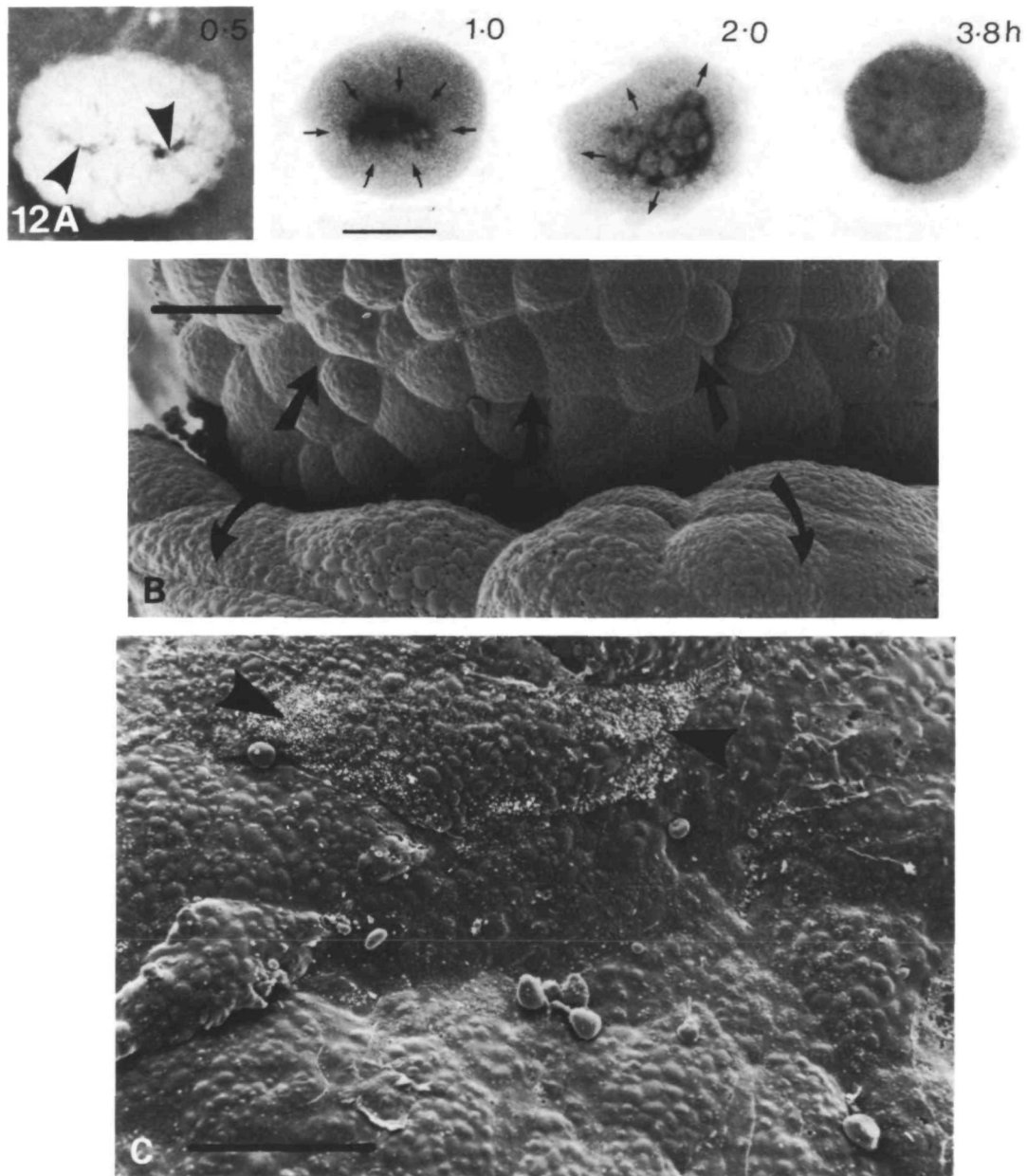


Fig. 12. Light micrographs from a time-lapse film show movements in an explant of the bottle cell region of a late blastula from 0.5 to 3.8 h in culture (A). A small blastoporal pigment line (pointers) has formed; the companion control was at stage 10. After 1 h in culture, the bottle cell area contracts centrally and turns inward (arrows) to form a pit with the condensed, darkly pigmented blastoporal pigment line at its bottom and with the unpigmented, basal ends of the bottle cells turned uppermost (toward the viewer) where they form the margin of the pit; the control was at stage 10.25. After 2 h, the blastoporal pigment line has begun to dissipate as the bottle cells respread (arrows); the control was at stage 11. After 3.8 h in culture, the bottle cells have completely respread and the blastoporal pigment line has dissipated; the control was at stage 11.5. An SEM shows the smaller, epithelial cells derived from the marginal zone, emerging from the pit (straight arrows) as they respread (B). The larger, vegetal cells also turn outward (curved arrows). A high magnification SEM (C) shows partially respread bottle cells with uneven distribution of microvilli on their apices (pointers) at a stage of respreading equivalent to that shown in C. Magnifications: A, $\times 55$, bar, 0.2 mm; B, $\times 325$, bar, 50 μm ; C, $\times 450$, bar, 50 μm .

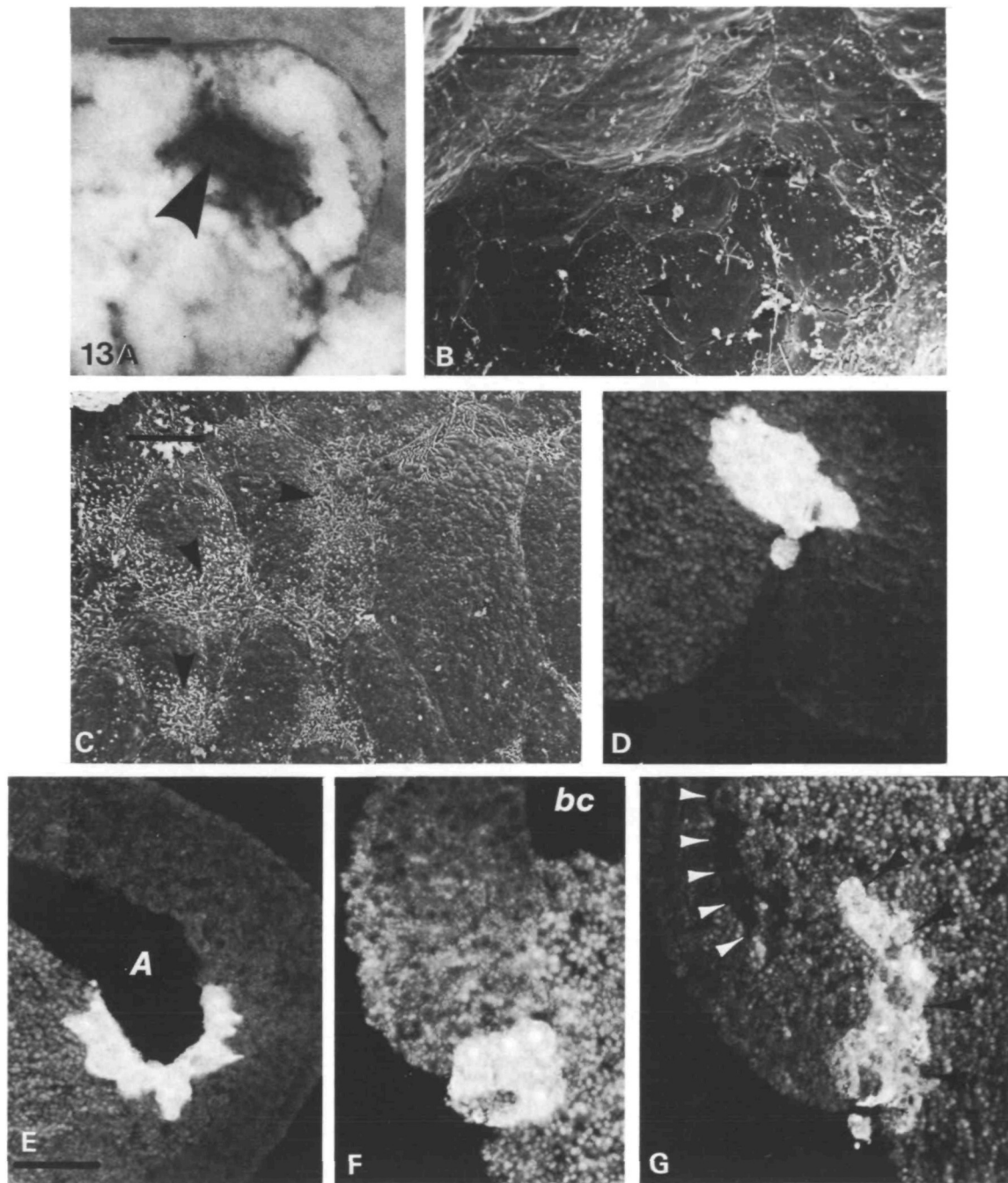


Fig. 13. A light micrograph shows the blind, anterior end of the archenteron (pointer) of a fixed and dissected stage-11 embryo, viewed from the posterior (A). The grey cells are nearly respread bottle cells, some of which retain pigment. SEM shows the respread apices and unevenly distributed microvilli (pointers) on cells at the anterior dorsal (B) and anterior ventral (C) aspects of the archenteron tip. Prospective bottle cells from FDA-labelled embryos were grafted to unlabelled embryos in the position shown in Fig. 4A. A midsagittal epifluorescence micrograph of the early gastrula shows the resulting bottle cells extending from the depth of the blastoporal groove (D), and a similar micrograph of the early neurula shows these cells respread to form a large area in the anterior wall of the archenteron (E). The animal pole is to the right in both micrographs. Prospective bottle cells and the deep cells underlying them were grafted from labelled to unlabelled embryos in the position shown in Fig. 4A. Epifluorescence micrographs show the position of the labelled cells after grafting at stage 9 (F) and after the bottle cells have formed at stage 10+ (G). Dorsal is to the left in both micrographs. The blastocoel (*bc*) is indicated and interface between the newly involuted mesoderm and the outer gastrula wall is outlined with small pointers. The labelled deep cells are displaced inwardly and anteriorly to form the leading edge of the mesodermal mantle (large pointers). Magnifications: A, $\times 44$, bar 0.2 mm; B, $\times 850$, bar 25 μm ; C, $\times 470$, bar 25 μm ; D–F, $\times 129$, bar 100 μm .

Movement of subjacent deep cells during bottle cell formation

What happens to the deep cells that originally lie subjacent to the prospective bottle cells, when this large area of epithelium contracts vegetally to form the much smaller area of the BPL (Fig. 4)? To answer this question, we grafted the prospective bottle cells and the subjacent deep cells from FDA-labelled embryos to unlabelled embryos prior to bottle cell formation (site indicated by shading in Fig. 4A). The grafted cells form a cuboid plug prior to bottle cell formation (Fig. 13F). After bottle cell formation, the subjacent deep cells are displaced inward and toward the animal pole in an arc that constitutes the tongue of prospective mesoderm that leads the involution of the mesodermal mantle (Fig. 13G).

Discussion

What behaviour is intrinsic to Xenopus bottle cells?

Our results suggest that apical constriction is an intrinsic motile activity of the forming bottle cells and that its strength is uniform in all directions. In contrast, the apical-basal elongation and the anisotropic shape of the apices are results of the anisotropic mechanical resistance of adjacent tissues. It is possible that an endogenous tendency to elongate in the apical-basal direction does exist, as it does in urodeles (Holtfreter, 1944), but is not sufficiently robust to survive our culture conditions. A number of processes may be involved in producing these cell shape changes (Baker, 1965; Perry & Waddington, 1966; Burnside, 1973; Viamontes *et al.* 1979), including modulation of the cell cycle (Hendrix & Zwaan, 1974; Smith & Schoenwolf, 1987) and differential rates of traction between cells (Jacobson *et al.* 1986).

Although nonuniform contraction is not an intrinsic property of amphibian bottle cells, it is an intrinsic property of the flask cells during *Volvox* inversion (Viamontes *et al.* 1979). To form a groove instead of a pit, either the apical contraction must be anisotropic as in *Xenopus* gastrulation and *Volvox* inversion (Viamontes *et al.* 1979) or the component cells must rearrange, as in amphibian neurulation (Jacobson & Gordon, 1976).

The respreading behaviour appears to be an intrinsic property of bottle cells, since it occurs in the same fashion and with the same timing among bottle cells isolated in culture. The disappearance of bottle cells has been attributed to cell death (see Keller, 1986). Here, however, we show that the bottle cells of *Xenopus* do not die but respread to form the peripheral wall of the archenteron, as previously suggested (Keller, 1975, 1981), and that they persist in this location at least until the early tadpole stage.

Apical constriction of bottle cells interacts with surrounding tissues to initiate involution of the IMZ

The effect of the intrinsic, isotropic contraction of the bottle cell apices is modulated by interaction with surrounding tissues in a way that initiates involution of the IMZ. The initial constriction of the bottle cells results in displacement of the IMZ vegetally rather than displacement of the vegetal region animally (Fig. 14), probably because of the greater stiffness or the greater thickness of the latter. As bottle cells develop a complete circle, they generate a hoop-stress around the vegetal cell mass. The vegetal cells resist this circumferential squeezing, and thus the intrinsically isotropic contraction of the bottle cell apices is directed primarily in the animal-vegetal direction, resulting in more effective vegetal displacement of the outer IMZ. The little circumferential contraction that does occur results in movement of the bottle cell area directly inward, squeezing the vegetal cell mass just below the IMZ (Fig. 14B). Also, the formation of the hoop-stress near the vegetal pole of the spherical embryo tends to pull the hoop farther toward the vegetal pole. This factor, in addition to the greater stiffness or thickness of the vegetal region, may ensure that the IMZ moves toward the vegetal region, rather than the other way round. The fact that there is a transition from an initial behaviour in which both the IMZ and the vegetal region move toward the bottle cells, the former more than the latter, to a later situation in which both regions move vegetally, argues that the geometric factor of hoop-stress overshadows the relative stiffness of the IMZ and vegetal regions in determining the effect of bottle cell formation on adjacent tissues. The overall effect of the hoop-stress is a significant constriction of the vegetal region and movement of the vegetal-most sector of the IMZ inward (Fig. 14B).

The apical constriction wedges cytoplasm basally and results in bending of the epithelial sheet in the fashion described by Lewis (1947) and Odell *et al.* (1981). If the IMZ and vegetal endoderm respond alike, a symmetrical groove should be formed, but instead, the IMZ is pushed outward and downward (Fig. 14B), perhaps because the vegetal region is less deformable. We note that uniform apical constriction would yield a pit, instead of a groove, but the vegetal endodermal mass provides resistance to the circumferential component of the intrinsically uniform contraction.

As bottle cells form, the deep mesoderm associated with them is displaced inward and upward, initiating involution (Fig. 14B,C). These cells form the leading edge of the mesodermal mantle. Whether this deep cell behaviour is a passive movement resulting directly from the mechanical effects of bottle cell

formation, or whether it is an active behaviour, either induced by bottle cell formation or independently controlled, is not clear.

The planar stretching of the outer, epithelial layer of the marginal zone vegetally, the squeezing of bottle cell cytoplasm basally to bend the epithelium,

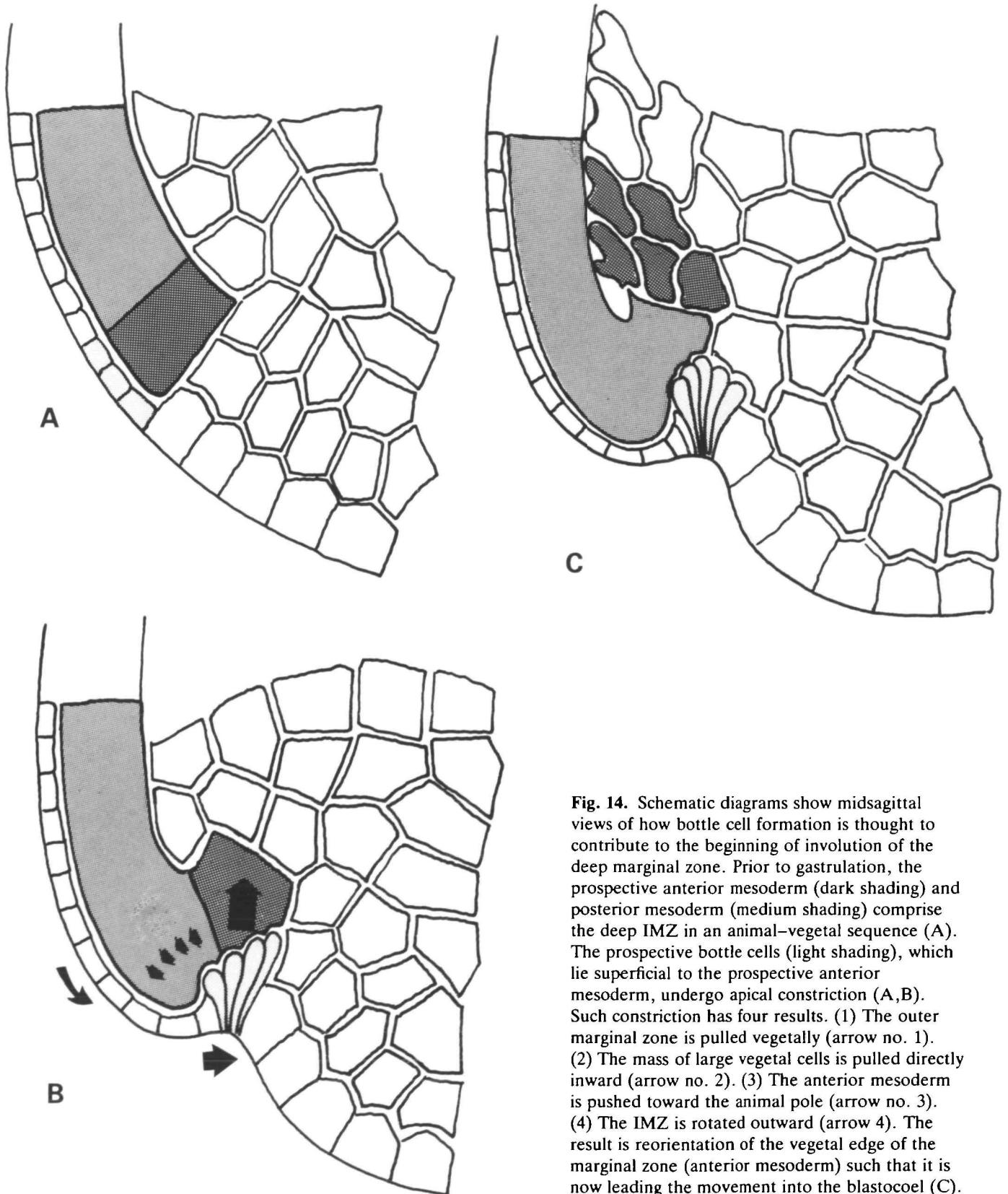


Fig. 14. Schematic diagrams show mid-sagittal views of how bottle cell formation is thought to contribute to the beginning of involution of the deep marginal zone. Prior to gastrulation, the prospective anterior mesoderm (dark shading) and posterior mesoderm (medium shading) comprise the deep IMZ in an animal-vegetal sequence (A). The prospective bottle cells (light shading), which lie superficial to the prospective anterior mesoderm, undergo apical constriction (A,B). Such constriction has four results. (1) The outer marginal zone is pulled vegetally (arrow no. 1). (2) The mass of large vegetal cells is pulled directly inward (arrow no. 2). (3) The anterior mesoderm is pushed toward the animal pole (arrow no. 3). (4) The IMZ is rotated outward (arrow 4). The result is reorientation of the vegetal edge of the marginal zone (anterior mesoderm) such that it is now leading the movement into the blastocoel (C).

the movement of the deep cells subjacent to the bottle cells inward and upward and the hoop-stress, acting to move vegetal region inward to a position more easily over-ridden by the IMZ, act in concert to produce a rolling of the IMZ that initiates its involution (Fig. 14).

Relation to convergence and extension of the IMZ

Bottle cell formation probably functions, along with the invasive behaviour of the prospective head mesoderm (Schechtman, 1942), to reorient the converging and extending material of the marginal zone (Keller, 1984; Keller *et al.* 1985a,b). If this does not occur, exogastrulation results as the converging and extending tissue is misoriented and forms long excrescences that extend outward into the medium (see Keller, 1986; Keller & Danilchik, 1988). We do not know the relative contributions of each process, whether both are necessary, or whether either alone is sufficient to initiate involution.

Not all bottle-shaped cells have the same behaviour or morphogenetic function

Xenopus bottle cells are endodermal and remain part of the superficial, epithelial layer of cells (also see Keller, 1975) whereas those of the lateral and ventral regions of the Mexican axolotl gastrula, and perhaps those of other urodelean gastrulae as well, are prospective mesodermal cells, which ingress to form a deep population of mesenchymal cells (Lundmark, 1986). As a result, they have more in common with the bottle-shaped cells in the primitive streak of the chick than with *Xenopus* bottle cells. Those in *Xenopus* appear to function by generating tension, bending a sheet and later respreading; the axolotl bottle cells function in the same way initially, but then lose their epithelial character and invade the gastrula interior. The basal ends of cultured bottle cells of some amphibians show invasive behaviour under some conditions (Holtfreter, 1943b). Although *Xenopus* bottle cells do not show signs of protrusive activity when in the bottle-shaped form (Keller & Schoenwolf, 1977), they may do so during respreading, a period in which they move with respect to adjacent tissues as they expand the margin of the archenteron beyond its initial position (Keller, 1975, 1981; also see Nieuwkoop & Florshutz, 1950; Nieuwkoop & Faber, 1967).

The relationship of yolk and bottle cell function to the reliability of gastrulation

Our results suggest that displacement of the bottle cells towards the equator in eggs with relatively large vegetal (subblastoporal) regions would make them less effective in reorienting the IMZ in the first half of gastrulation. Thus the powerful convergence and

extension movements of the IMZ, which normally close the blastopore (Schechtman, 1942; Keller *et al.* 1985a,b), should be misdirected and a higher frequency of exogastrulation should result (see Keller, 1986). Under laboratory conditions, some *Xenopus* spawnings yield large, yolky eggs in which the bottle cells form at 75° or 80° instead of the usual 45°–55°. Such animals show bottle cell profiles as predicted by the simulations, a failure of marginal zone rotation, and exogastrulation (R. E. Keller, unpublished work). Egg size and yolk content varies among species of amphibians, depending on their reproductive strategy (see Salthe & Duellman, 1973; Kaplan, 1980) and some have quite large, yolky eggs (del Pino & Escobar, 1981; del Pino & Elinson, 1983). We expect that the bottle cells in these large yolky amphibian eggs have a location or mechanism of function different from that in *Xenopus*, if they exist at all.

Significance for analysis of cell function in morphogenesis

The bottle cells raise several points concerning the relation of cell behaviour to morphogenesis. First, the behaviour of the bottle cells reminds us that it is as much the context of a cell behaviour, and its spatial and temporal patterning, as it is the behaviour itself, that is important in generating specific morphogenetic events (see Holtfreter, 1939). Basic operations of cells, such as contraction and adhesion, are essential but general properties that explain little about morphogenesis in themselves. In amphibian gastrulation, as in amphibian neurulation (Jacobson & Gordon, 1976), the forces generated by individual cells may interact in complex ways with external factors to reshape tissues. Second, the role of cell shape in deforming cell sheets must be considered in terms of those changes that occur within the plane of the sheet as well as in profile. Finally, the bottle cells demonstrate that even a dramatic change in cell shape does not necessarily imply a far-reaching and universal role in morphogenesis. The bottle cells of *Xenopus* act locally rather than globally; they act as part of a system of interacting processes rather than the sole driving force of gastrulation and they appear to perform different functions at different stages of development. Moreover, these functions differ from those of their similarly shaped counterparts in other systems.

We thank Paul Tibbetts for his technical work and Paul Wilson for his insightful comments and corrections. This research was done under the support of NIH grant HD18979 to Ray Keller and an NSF Predoctoral Fellowship to Jeff Hardin.

References

- BAKER, P. (1965). Fine structure and morphogenetic movements in the gastrula of the treefrog, *Hyla regilla*. *J. Cell Biol.* **24**, 95–116.
- BURNSIDE, B. (1973). Microtubules and microfilaments in amphibian neurulation. *Am. Zool.* **13**, 989–1006.
- BUYTENDIJK, F. J. J. & WOERDEMAN, M. W. (1927). Die physico-chemischen Erscheinungen während der Entwicklung. *Wilhelm Roux' Arch. EntwMech. Org.* **112**, 387–410.
- CHENG, L. Y. (1987a). Deformation analysis in cell and developmental biology. Part I: Formal methodology. *J. Biomech.* **109**, 10–17.
- CHENG, L. Y. (1987b). Deformation analysis in cell and developmental biology. Part II: Mechanical experiments on cells. *J. Biomech.* **109**, 18–24.
- COOKE, J. (1975). Local autonomy of gastrulation movements after dorsal lip removal in two anuran amphibians. *J. Embryol. exp. Morph.* **33**, 147–157.
- DEL PINO, E. & ELINSON, R. (1983). A novel development pattern for frogs: gastrulation produces an embryonic disk. *Nature, Lond.* **306**, 589–591.
- DEL PINO, E. & ESCOBAR, B. (1981). Embryonic stages of *Gastrotheca riobambae* (Fowler) during maternal incubation and comparison of development with that of the egg-brooding hylid frogs. *J. Morph.* **167**, 277–295.
- ETTENSohn, C. (1984). Primary invagination of the vegetal plate during sea urchin gastrulation. *Am. Zool.* **24**, 571–588.
- ETTENSohn, C. (1985). Mechanisms of epithelial invagination. *Q. Rev. Biol.* **60**, 289–307.
- GILLESPIE, J. I. (1983). The distribution of small ions during the early development of *Xenopus laevis* and *Ambystoma mexicanum* embryos. *J. Physiol., Lond.* **344**, 359–377.
- GIMLICH, R. L. & BRAUN, J. (1985). Improved fluorescent compounds for tracing cell lineage. *Dev Biol.* **109**, 509–514.
- GIMLICH, R. L. & COOKE, J. (1984). Cell lineage and induction of second nervous systems in amphibian development. *Nature, Lond.* **306**, 471–473.
- GUSTAFSON, T. & WOLPERT, L. (1967). Cellular movement and contact in sea urchin morphogenesis. *Biol. Rev.* **42**, 442–498.
- HARDIN, J. D. & CHENG, L. Y. (1986). The mechanisms and mechanics of archenteron elongation during sea urchin gastrulation. *Dev Biol.* **115**, 490–501.
- HENDRIX, R. W. & ZWAAN, J. (1974). Cell shape regulation and cell cycle in embryonic lens cells. *Nature, Lond.* **247**, 145–147.
- HILFER, S. R. & HILFER, E. S. (1983). Computer simulation of organogenesis: an approach to the analysis of shape changes in epithelial organs. *Dev Biol.* **97**, 444–453.
- HOLTFRETER, J. (1939). Gewebeaffinität, ein Mittel der embryonalen Formbildung. *Arch. exp. Zellforsch. Besonders Gewebequecht* **23**, 169–209.
- HOLTFRETER, J. (1943a). Properties and function of the surface coat in amphibian embryos. *J. exp. Zool.* **93**, 251–323.
- HOLTFRETER, J. (1943b). A study of the mechanics of gastrulation. Part I. *J. exp. Zool.* **94**, 261–318.
- HOLTFRETER, J. (1944). A study of the mechanics of gastrulation. Part II. *J. exp. Zool.* **95**, 171–212.
- JACOBSON, A. & GORDON, R. (1976). Changes in the shape of the developing vertebrate nervous system analyzed experimentally, mathematically, and by computer simulation. *J. exp. Zool.* **197**, 191–246.
- JACOBSON, A. G., OSTER, G. F., ODELL, G. M. & CHENG, L. Y. (1986). Neurulation and the cortical tractor model for epithelial folding. *J. Embryol. exp. Morph.* **96**, 19–49.
- KAPLAN, R. H. (1980). The implications of ovum size variability for offspring fitness and clutch size within several populations of salamanders (*Ambystoma*). *Evolution* **34**, 51–64.
- KARFUNKEL, P. (1974). The mechanisms of neural tube formation. *Int. Rev. Cytol.* **38**, 245–271.
- KELLER, R. E. (1975). Vital dye mapping of the gastrula and neurula of *Xenopus laevis*. I. Prospective areas and morphogenetic movements of the superficial layer. *Dev Biol.* **42**, 222–241.
- KELLER, R. E. (1978). Time-lapse cinemicrographic analysis of superficial cell behavior during and prior to gastrulation in *Xenopus laevis*. *J. Morph.* **157**, 223–248.
- KELLER, R. E. (1981). An experimental analysis of the role of bottle cells and the deep marginal zone in gastrulation of *Xenopus laevis*. *J. exp. Zool.* **216**, 81–101.
- KELLER, R. E. (1984). The Cellular Basis of Gastrulation in *Xenopus laevis*: Active, Postinvolution Convergence and Extension by Mediolateral Interdigitation. *Am. Zool.* **24**, 589–603.
- KELLER, R. E. (1986). The Cellular Basis of Amphibian Gastrulation. In *Developmental Biology: A Comprehensive Synthesis*, vol. 2, *The Cellular Basis of Morphogenesis* (ed. L. Browder), pp. 241–327. New York: Plenum Press.
- KELLER, R. E. & DANILCHIK, M. V. (1988). Regional expression, pattern, and timing of convergence and extension during gastrulation of *Xenopus laevis*. *Development* **103**, 193–209.
- KELLER, R. E., DANILCHIK, M., GIMLICH, R. & SHIH, J. (1985a). Convergent extension by cell intercalation during gastrulation of *Xenopus laevis*. In *Molecular Determinants of Animal Form* (ed. G. M. Edelman), *UCLA Symp. Mol. Cell Biol.*, vol. 31, pp. 111–141. New York: Alan R. Liss, Inc.
- KELLER, R. E., DANILCHIK, M., GIMLICH, R. & SHIH, J. (1985b). The function and mechanism of convergent extension during gastrulation of *Xenopus laevis*. *J. Embryol. exp. Morph.* **89**, Supplement, 185–209.
- KELLER, R. E. & SCHOENWOLF, G. C. (1977). An SEM study of cellular morphology, contact, and arrangement, as related to gastrulation in *Xenopus laevis*. *Wilhelm Roux' Arch. devl Biol.* **182**, 165–186.
- LEWIS, W. H. (1947). Mechanics of invagination. *Anat. Rec.* **97**, 139–156.
- LUNDMARK, C. (1986). Role of bilateral zones of ingressing superficial cells during gastrulation of

- Ambystoma mexicanum. *J. Embryol. exp. Morph.* **97**, 47–62.
- NIEUWKOOP, P. & FABER, J. (1967). *Normal Table of Xenopus laevis (Daudin)*. Second edition. Amsterdam: North-Holland Publishing Company.
- NIEUWKOOP, P. & FLORSHUTZ, P. (1950). Quelques caracteres speciaux de la gastrulation et de la neurulation de l'oeuf de *Xenopus laevis*, Daud. et de quelques autres Anoures. I ere partie. -Etude descriptive. *Archs Biol., Liege* **61**, 113–150.
- ODELL, G. M., OSTER, G., ALBERCH, P. & BURNSIDE, B. (1981). The mechanical basis of morphogenesis. I. Epithelial folding and invagination. *Devl Biol.* **85**, 446–462.
- PERRY, M. & WADDINGTON, C. H. (1966). Ultrastructure of the blastoporal cells in the newt. *J. Embryol. exp. Morph.* **15**, 317–330.
- RHUMBLER, L. (1902). Zur Mechanik des Gastrulationsvorganges, insbesondere der Invagination. Eine entwicklungsmechanische Studie. *Wilhelm Roux' Arch. EntwMech. Org.* **14**, 401–476.
- RUFFINI, A. (1925). *Fisogenia*. Milano: Francesco Vallardi.
- SALTHER, S. & DUELLMAN, W. E. (1973). *Evolutionary Biology of the Anurans* (ed. J. L. Vial), pp. 229–249. Columbia: University of Missouri Press.
- SCHECHEMAN, A. M. (1942). The mechanism of amphibian gastrulation. I. Gastrulation-promoting interactions between various regions of an anuran egg (*Hyla regilla*). *Univ. Calif. Publ. Zool.* **51**, 1–39.
- SCHOENWOLF, G. C. (1985). Shaping and bending of the avian neuroepithelium: Morphometric analysis. *Devl Biol.* **109**, 127–139.
- SCHROEDER, T. E. (1970). Neurulation in *Xenopus laevis*. An analysis and model based upon light and electron microscopy. *J. Embryol. exp. Morph.* **23**, 427–462.
- SMITH, J. L. & SCHOENWOLF, G. C. (1987). Cell cycle and neuroepithelial cell shape during bending of the chick neural plate. *Anat. Rec.* **218**, 196–206.
- STABLEFORD, L. J. (1949). The blastocoel fluid in amphibian gastrulation. *J. exp. Zool.* **112**, 529–546.
- VIAMONTES, G., FOCHTMANN, L. & KIRK, D. (1979). Morphogenesis of *Volvox*: Analysis of critical variables. *Cell* **17**, 537–550.
- ZWAAN, J. & PEARCE, T. L. (1971). Cell population kinetics in the chicken lens primordium during and shortly after its contact with the optic cup. *Devl Biol.* **25**, 96–118.

(Accepted 26 January 1988)